A GPR Agricultural Drainage Pipe Detection Case Study: Effects of Antenna Orientation Relative to Drainage Pipe Directional Trend

Barry J. Allred
USDA/ARS – Soil Drainage Research Unit, 590 Woody Hayes Drive, Room 234, Columbus, Ohio, USA 43210
Email: Barry.Allred@ars.usda.gov

ABSTRACT

Locating buried drainage pipes is a difficult task confronting farmers and land improvement contractors, especially in the Midwest U.S., where the removal of excess soil water using subsurface drainage systems is a common farm practice. Enhancing the efficiency of soil water removal on land containing a functioning subsurface drainage system typically involves installing new drain lines between the old ones. Before this approach can be attempted, the older drain lines have to be mapped. Previous research supports the feasibility of using ground penetrating radar (GPR) to find buried agricultural drainage pipes. However, one aspect of GPR drainage pipe location and assessment needing further investigation is the GPR pipe response effects associated with GPR antenna orientation relative to drainage pipe directional trend.

A field research study was carried out at a specially designed test plot to evaluate the effect on GPR drainage pipe detection caused by the antenna-to-pipe orientation. Antenna orientations perpendicular and parallel to drain lines were tested using 250 MHz antennas. The GPR data were collected under moderately dry and very wet soil conditions. Overall study results indicated that there can be substantial differences in the strength of the GPR drainage pipe response for an antenna orientation perpendicular to a drain line versus an antenna orientation parallel to a drain line. Under moderately dry soil conditions, a GPR antenna orientation perpendicular to the drain line provided the best GPR drainage pipe response. Conversely, under very wet soil conditions, a GPR antenna orientation parallel to a drain line provided the best GPR drainage pipe response. Consequently, the findings indicated that on-site assessment of soil moisture conditions and knowledge of general drain line directional trend can guide the GPR system antenna set-up and formulation of a GPR survey plan to improve GPR drainage pipe detection and assessment capabilities.

Introduction

A 1985 economic survey (Pavelis, 1987) showed that the states comprising the Midwest U.S. (Illinois, Indiana, Iowa, Ohio, Minnesota, Michigan, Missouri, and Wisconsin) had approximately 12.5 million hectares that contained subsurface drainage systems. Cropland accounts for the large majority of the Midwest U.S. areas that have buried drainage pipe networks. Farmers within this region often need to improve or repair pre-existing subsurface drainage pipe systems, but before this is done, drain lines have to be located and then a determination made as to whether they are functioning properly. Several investigations have documented the capability of ground penetrating radar (GPR) to find buried plastic or metal utility pipelines (LaFaleche *et al.,* 1991; Wensink *et al.,* 1991; Zeng and McMechan, 1997; Hayakawa and Kawanaka, 1998). The ElectroScience Laboratory at Ohio State University developed a GPR system capable of finding 60% of plastic utility pipes in 60% of the U.S. (Peters and Young, 1986). There has also been prior research specifically indicating that GPR can be effective in locating buried drainage pipes. Chow and Rees (1989) demonstrated the use of GPR to locate subsurface agricultural drainage pipes in the Maritime Provinces of Canada, while Boniak *et al.* (2002) and Allred *et al.* (2005a) showed that GPR could be employed to find drainage pipe beneath golf course greens and tees.

Ground penetrating radar surveys were conducted in southwest, central, and northwest Ohio at fourteen test plots (including the one used in this study). With respect to locating the total amount of pipe present at each site, this technology was shown to have an average

 DOI: 10.2113/JEEG18.1.55

effectiveness of 74%; with 100% of the pipe found at seven sites, 90% at one site, 75% at two sites, 50% at two sites, and 0% at two sites (Allred *et al.,* 2004; Allred *et al.,* 2005b; Allred and Redman, 2010). Based on this testing, GPR was shown to be reasonably successful in finding clay tile and corrugated plastic tubing (CPT) drainage pipe down to depths of around 1 m in a variety of different soil types. Allred *et al.* (2005b) additionally determined the impact of computer processing procedures, equipment attributes, site conditions, and field operations on GPR agricultural drainage pipe detection. Allred and Redman (2010) showed, given certain shallow hydrologic conditions, that GPR was capable of locating an isolated obstruction in a drainage pipe affecting water conveyance functionality.

The previous investigations clearly indicate the feasibility of using GPR to locate buried agricultural drainage pipes, and perhaps, under specific circumstances, also provide insight on drain line functionality. However, one aspect of GPR agricultural drainage pipe detection and functionality assessment needing further investigation is the GPR pipe response effects associated with GPR antenna orientation relative to drainage pipe directional trend. Research by Roberts and Daniels (1996), Radzevicius and Daniels (2000), and Streich *et al.* (2008) provide indications that the antenna orientation relative to the buried utility pipe directional trend can significantly impact the GPR pipe response. Specifically, Radzevicius and Daniels (2000) conclude that for relatively small diameter cylinders buried beneath the ground surface in which the dielectric constant of the cylinder is substantially less that the dielectric constant of the surrounding soil, a GPR transmitting/receiving antenna orientation perpendicular to the axis of the buried cylinder will produce a stronger GPR response than a transmitting/receiving antenna orientation parallel to the axis of the buried cylinder. Conversely, if the dielectric constant of the cylinder is substantially greater than the dielectric constant of the surrounding soil, then a GPR transmitting/receiving antenna orientation parallel to the axis of the buried cylinder will produce a stronger GPR response than a transmitting/receiving antenna orientation perpendicular to the axis of the buried cylinder.

Ground penetrating radar systems often have the transmitting and receiving antennas placed parallel to one another and enclosed together within a single housing. The GPR equipment set-up most commonly employed has the transmitting and receiving antennas positioned perpendicular to the direction along which GPR measurements are collected. Most GPR systems also have the capability of positioning the transmitting and receiving antennas parallel to the direction along which GPR measurements are collected. Therefore, given general knowledge of the directional trend for drain lines in a farm field (information that is often available or can be deduced), GPR data can be collected with antennas either parallel or perpendicular to the drainage pipes. The antenna-to-pipe orientation (parallel or perpendicular) chosen for GPR drainage pipe detection and functionality assessment will be the one known to produce the strongest GPR pipe response for particular farm field conditions.

A field research study was initiated to evaluate the GPR agricultural drainage pipe response effects caused by antenna orientation relative to drainage pipe directional trend. To accomplish the research, a GPR system with 250 MHz antennas was tested under moderately dry and very wet soil conditions at a specially designed test plot containing an open, totally unobstructed drain line; a completely obstructed drain line, plugged near its midpoint; a soil-filled drain line; a severed, partially obstructed drain line; and two pre-existing drain lines of unknown construction and condition. Ground penetrating radar data were collected with antennas parallel to the drainage pipes and with antennas perpendicular to the drainage pipes. The guiding research hypothesis can be stated as follows, "The strength of the GPR agricultural drainage pipe response depends significantly on the antenna-to-pipe orientation in combination with soil moisture conditions."

Experimental Site, Equipment, and Procedures

Test Plot Description

A test plot constructed in 2006 for a previous study (Allred and Redman, 2010) was employed for this research project. The test plot is located at the Ohio State University - Waterman Agricultural and Natural Resources Laboratory in Columbus, Ohio. The dimensions of the test plot are 12.2 m east-west by 24.4 m north-south. Trenching equipment was used to install four drain lines at this test plot. After drain line installation, the entire test plot was tilled to a depth of 0.3 m. Following tillage, a short grass cover was developed and maintained across the test plot. Figures 1(a) and 1(b) are schematic profiles of an installed drain line. The corrugated plastic tubing (CPT) drainage pipe that was used, because of the corrugations, had a minimum inside diameter of 0.10 m and a maximum outside diameter of 0.12 m, even though the wall thickness is only 0.001 m. The small amount of clay tile drainage pipe utilized had a wall thickness of 0.01 m, a consistent inside diameter of 0.10 m, and a consistent outside diameter of 0.12 m. The diameters of the drainage pipe used for this study were similar to those that have been most commonly used in agricultural practice. Clay tile

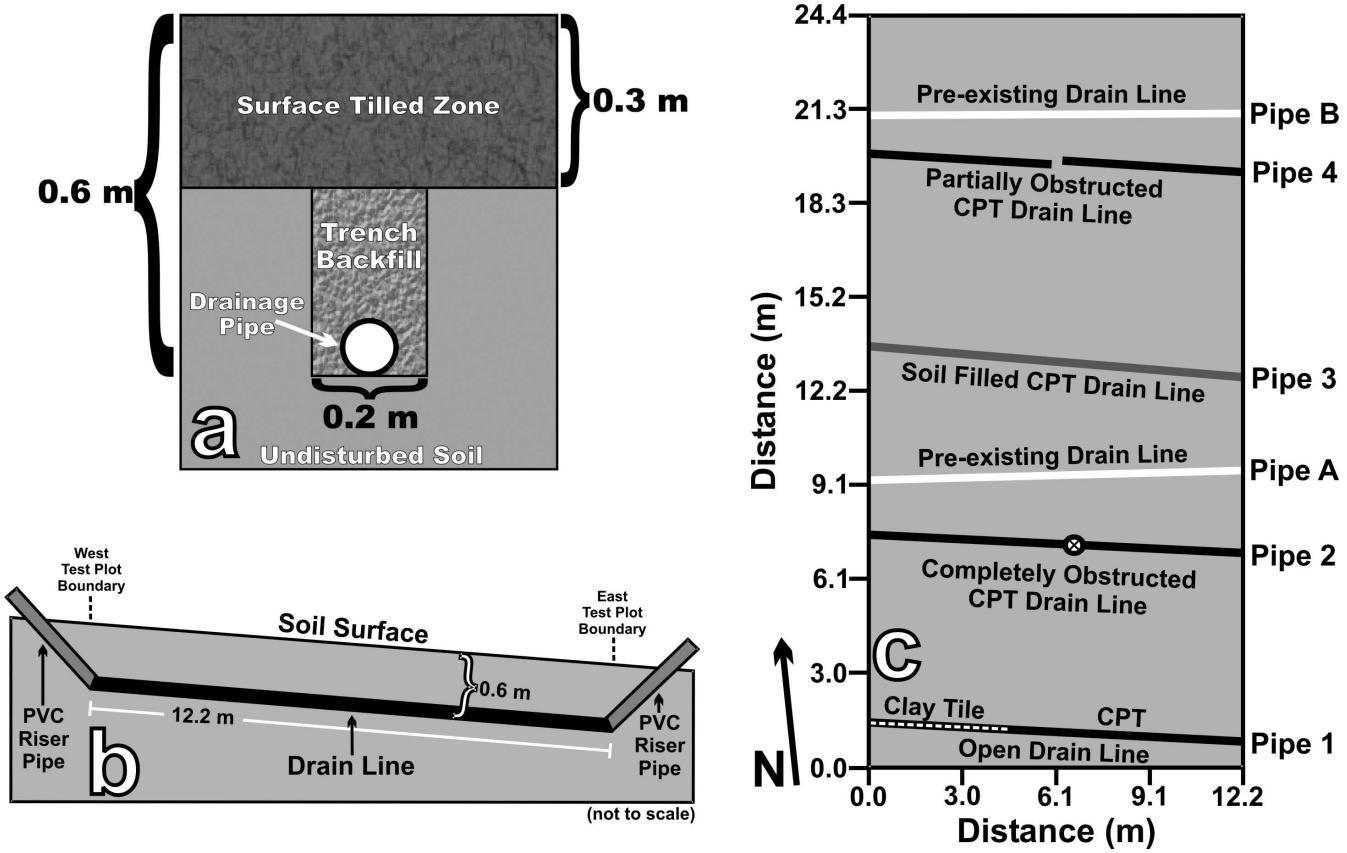

Figure 1. Test plot schematics: a) profile oriented perpendicular to drainage pipe direction, b) profile along the length of a recently installed drain line, c) map showing locations for recently installed drain lines (Pipes 1, 2, 3, and 4) and pre-existing drain lines (Pipes A and B).

drainage pipe was installed up until the late 1960's, after which CPT drainage pipe became the type normally installed in agricultural settings. Each drain line had a length of 12.2 m. The backfilled trenches had a width of 0.2 m and a depth of approximately 0.6 m (Fig. 1(a)). A backfilled trench without drainage pipe, to be used for background assessment, was not included within this test plot because previous investigations indicated that the backfilled trench itself did not produce a substantial ground penetrating radar response.

Within typical Ohio agricultural settings, the tilled zone thickness is 0.3 m or less, and the trench where a drainage pipe is placed usually has a width between 0.2 to 0.5 m. Although somewhat shallow, the test plot trench depth for the installed drain lines was within the depth range that drainage pipe in Ohio are normally buried (0.5 to 1.0 m). Polyvinyl chloride (PVC) riser pipe (0.10 m inside diameter) were extended from both ends of a drain line to a height of 0.3 m above the ground surface (Fig. 1(b)), thereby permitting water to be easily added or removed from a drain line and to also allow determination of the presence or absence of water in the drain lines (Fig. 1(b)). The soil surface and the drain line itself slope downwards approximately 0.2 m from the west to east ends of a drain line.

A schematic map of the test plot showing drain line locations is provided in Fig. 1(c). With respect to the four recently installed drain lines, one is a clay tile to CPT drain line completely open to flow (Pipe 1); one is comprised of CPT with an isolated obstruction near the midpoint, completely preventing through-flow of water (Pipe 2); one is comprised of CPT, but filled with soil (Pipe 3); and one is comprised of CPT but severed near its midpoint, producing a partial obstruction to water flow (Pipe 4). Although Pipe 3 originally was totally filled with soil, previous GPR field and computer modeling research results (Allred and Redman, 2010) indicated that there was probably some soil settlement within the pipe, which resulted in a small portion at the top of the pipe being open and not soil-filled. Furthermore, Allred and Redman (2010) unexpectedly found two pre-existing drain lines at the test plot (Pipe A and Pipe B) of unknown construction and condition buried at a depth near 0.6 m (Fig. 1(c)).

The soil covering the test plot was derived from glacial till and is part of the Crosby Series (fine, mixed,

mesic Aeric Ochraqualfs). Soil samples obtained from the test plot were classified as clay loam based on particle size analysis (Wray, 1986). Test plot topography was mapped with real-time kinematic (RTK) global positioning system (GPS) technology using a Topcon Positioning Systems, Inc. (Livermore California), HiPer XT Wireless RTK GPS. The ground surface of the test plot slopes downward in a fairly uniform manner from the southwest corner to the northeast corner. The total elevation difference between the southwest and northeast corners is 0.55 m.

Modification and Monitoring of Test Plot Shallow Hydrologic Conditions

Ground penetrating radar (GPR) measurements and other field data were obtained over three days, August 12–14, 2009. In the ten days prior to August 12, there was very little rainfall, less than 1 cm in total, and no rainfall during the test period itself (National Climate Data Center, 2009). Therefore, test plot soil conditions on August 12, 2009 were moderately dry. Following the first collection effort for GPR measurements and other field data, which occurred on the morning of August 12, 2009, a sprinkler irrigation system was employed to apply water to the test plot surface over the next 20 hours. Once the sprinkler irrigation system was turned off on the morning of August 13, 2009, GPR measurements and other field data were again collected at the test plot. The test plot was then allowed to drain from the morning of August 13, 2009 through the morning of August 14, 2009, after which the final sets of GPR measurements and field data were obtained.

Soil surface water content was measured on August 12, 13, and 14, 2009. On August 12, prior to initiation of sprinkler irrigation, time domain reflectometry (TDR) methods were used to determine near-surface (0.0-m to 0.2-m depth) soil volumetric water content values. The TDR soil volumetric water content measurements were obtained at the center and corners of the test plot using a Spectrum Technologies, Inc. (East Plainfield, Illinois), Field Scout TDR-300. However, a malfunction of the TDR equipment on August 12 necessitated the collection of soil samples for all further soil surface water content determinations. Near-surface soil samples (0.0 m to 0.15 m) used for determining soil water content were collected at the southwest corner, center, and northeast corner of the test plot on each day; August 12 before initiation of sprinkler irrigation, August 13 once sprinkler irrigation was discontinued, and the morning of August 14, after the test plot had drained for approximately 24 hours. Gravimetric soil water content values (weight of water divided by the weight of dry soil) were obtained by weighing all soil samples before and after 24 hours of oven drying at 105 °C. To further evaluate test plot shallow hydrologic conditions, a 3.5-m long, 0.02-m diameter flexible PVC pipe with its outside surface coated with water-indicating paste (Kolor Kut Water Finding Paste, Kolor Kut Products Company, Houston, Texas) was inserted via the PVC riser pipes into both ends of each recently installed drain line to verify the presence or absence of water within the drain lines. As with the soil sampling, drain line probing for presence or absence of water was carried out on August 12 before initiation of sprinkler irrigation, August 13 once sprinkler irrigation was discontinued, and the morning of August 14, after the test plot had drained for approximately 24 hours.

Soil electrical conductivity measurements often provide insight on shallow hydrologic conditions and GPR performance. Low values for soil electrical conductivity can indicate dry soil conditions and a greater GPR signal penetration depth, while conversely, high values for soil electrical conductivity can indicate wet soil conditions and less GPR signal penetration depth. Consequently, electromagnetic induction methods were employed, using a Geophex, Ltd. (Raleigh, North Carolina), GEM-2 ground conductivity meter, to obtain apparent soil electrical conductivity (EC_a) measurements uniformly across the test plot. The GEM-2 was operated at a frequency of 14.6 kHz, with approximately ten measurements taken per second. The co-planer transmitter/receiver intercoil spacing is 1.66 m, and during use, the GEM-2 was held approximately 1 m above the ground surface and oriented in the vertical dipole mode (horizontal co-planer coil configuration), thereby providing an EC_a investigation depth of approximately 1.5 m (based on McNeill, 1980). The GEM-2 equipment design compensates for internal temperature change, and periodic electromagnetic induction readings obtained with a ferrite rod placed on the GEM-2 at a specified location ensured that the GEM-2 remained calibrated and did not require calibration adjustment. Again, as with the soil sampling and the drain line probing for presence or absence of water, test plot EC_a values were obtained on August 12 before initiation of sprinkler irrigation, August 13 once sprinkler irrigation was discontinued, and the morning of August 14, after the test plot had drained for approximately 24 hours.

Ground Penetrating Radar Equipment and Equipment Settings

A Sensors & Software Inc. (Mississauga, Ontario, Canada), Noggin^{plus} ground penetrating radar (GPR) unit with 250 MHz antennas and an integrated odometer was used to study GPR drainage pipe responses. The GPR unit with 250 MHz center frequency antennas was chosen for use in this study because of its drainage pipe detection success in previous

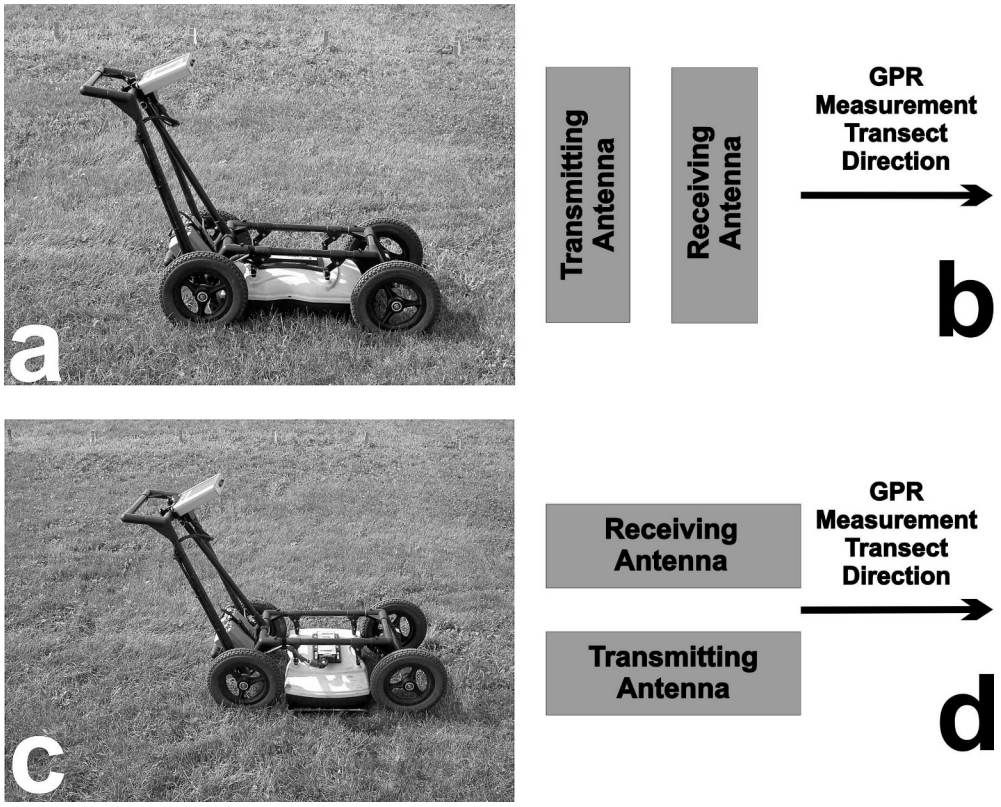

Figure 2. GPR system antenna configurations used in this study: a) photo of GPR system with antennas oriented perpendicular to measurement transect direction, b) schematic further emphasizing the antenna orientation depicted in the Fig. 1(a) photo, c) photo of GPR system with antennas oriented parallel to measurement transect direction, and d) schematic further emphasizing the antenna orientation depicted in the Fig. 1(c) photo.

investigations (Allred *et al.,* 2004; Allred *et al.,* 2005a; Allred *et al.,* 2005b; Allred and Redman, 2010). For this GPR unit, the separation distance between the 250 MHz transmitter and receiver antennas was 0.28 m. This antenna separation distance is optimal for minimizing attenuation losses and maximizing target coupling and system dynamic range. In addition, this GPR system was set-up to have a 0.05-m separation distance between measurement points on a transect, and 32 signal traces were averaged (stacked) at each measurement point, with a 0.4-ns sampling interval along each signal trace. Ground penetrating radar data were collected with the transmitting and receiving antennas perpendicular to the GPR measurement transect direction (Figs. 2(a) and 2(b)) and with the transmitting and receiving antennas parallel to the GPR measurement transect direction (Figs. 2(c) and 2(d)). Consequently, GPR antenna orientations both parallel and perpendicular to the test plot drain lines were investigated.

Ground Penetrating Radar Test Plot Data Collection

Ground penetrating radar data were collected on three separate days, August 12, August 13, and August 14, 2009. On all three days, GPR measurements were first obtained along two series of south-to-north transects, with each series beginning at the west test plot boundary and finishing at the east test plot boundary. The GPR measurement transect grid was marked out on the test plot using measuring tape and flagged wooden stakes. For the first south-to-north series of transects, the GPR antennas were oriented parallel to the drain lines, while the second series in the pair had antennas oriented perpendicular to the drain lines. All eleven south-to-north GPR transects in a series were 24.4 m in length and spaced 1.2 m apart. While this 1.2-m spacing distance between transects does not provide complete GPR spatial coverage to detect all small isolated targets, it is more than adequate for imaging of drain lines that extend across the test plot. Along with the two south-north GPR transect series, two additional series of GPR data were obtained along four 12.2-m west-east transects oriented directly over top and along trend with the four recently installed drain lines (one series with antenna orientation parallel and one series perpendicular relative to the Pipes 1, 2, 3, and 4). Locations for individual GPR measurements

Table 1. Average and standard deviation (in parenthesis) of test plot soil water content and soil electrical conductivity.

Data collection date	Soil gravimetric water content (dimensionless)	Soil volumetric water content (dimensionless)	Apparent soil electrical conductivity (EC_a) (mS/m)
August 12, 2009	0.116 (0.009)	0.184 (0.031)	17.65 (2.16)
August 13, 2009	0.297 (0.020)	0.470* (0.032*)	30.68 (4.51)
August 14, 2009	0.271 (0.007)	0.431* (0.012*)	27.57 (2.39)

*Estimated value based on calculated August 12 ratio of volumetric water content to gravimetric water content.

along any particular transect were determined with a highly accurate and precise odometer, which was an integrated component of the Noggin^{plus} GPR unit.

Ground Penetrating Radar Test Plot Data Processing

Ground penetrating radar time/depth profiles showing drainage pipe responses were generated for each transect. Computer processing of the GPR profiles required application of a signal saturation correction filter to remove low frequency noise, followed by signal gain (spreading and exponential compensation function with a starting value of 8.0, an attenuation of 20.0 decibels/m, and a maximum gain factor of 500). Amplitude maps were also produced from each test plot series of eleven south-to-north GPR measurement transects. The computer processing steps used to produce the GPR amplitude maps for this project included a signal saturation correction filter, signal trace enveloping, 2-D migration, and a spatial background subtraction filter. Signal trace enveloping converts signal wavelets having positive and negative components into ones that are unipolar and positive, thereby removing the oscillatory nature of radar signal wavelets (Sensors & Software Inc., 2009). Or, described in another way, the signal trace enveloping process makes all the negative components of a radar signal wavelet positive and then smoothes the wavelet outline. The 2-D migration step collapses hyperbolic responses to point targets. The spatial background subtraction filter suppressed flat-lying horizontal features. With GPR amplitude map processing, drainage pipes appeared as high amplitude, lightly shaded linear features.

Results and Discussion

Test Plot Shallow Hydrologic Conditions

On August 12, 2009, the first set of GPR data were collected prior to initiation of sprinkler irrigation. The near-surface soil volumetric water content across the test plot averaged only 0.184, as measured using time domain reflectometry (TDR) methods (Table 1). The near-surface soil gravimetric water content at the test plot averaged 0.116 based on oven drying of soil samples (Table 1). The relationship between soil volumetric water content, θ, and soil gravimetric water content, w, is given by:

$$\theta = w\left(\frac{\rho_b}{\rho_w}\right), \quad (1)$$

where ρ_b is the soil dry bulk density, and ρ_w is the density of water (Hillel, 1980). On August 12, with an average θ of 0.184 and an average w of 0.116, the calculated ρ_b/ρ_w ratio is 1.586. Because of a malfunction of the TDR probe, this ρ_b/ρ_w ratio of 1.586, along with Eq. (1), was in turn used to estimate soil volumetric water contents for August 13 and August 14 from the measured values of soil gravimetric water content.

The August 12 apparent soil electrical conductivity (EC_a) across the test plot averaged only 17.65 mS/m, with a standard deviation of 2.16 mS/m, as measured using the electromagnetic induction method (Table 1). The relatively low average EC_a indicated a fairly dry soil profile, while the small EC_a standard deviation implies that soil properties and conditions were fairly uniform across the test plot. Additionally, none of the four recently installed drain lines contained any water. A depleted near-surface soil water content, low EC_a values, and the absence of water in the drain lines, all indicate initial moderately dry test plot soil conditions with a water table level that was below the bottom of the recently installed drain lines (>0.6 m).

On August 13, 2009, the second set of GPR data was collected following 20 hours of intense sprinkler irrigation. The test plot's shallow hydrologic conditions were extremely wet with a saturated ground surface (small puddles of standing water). The estimated near-surface soil volumetric water content averaged 0.470 (Table 1). A relatively large test plot EC_a value of 30.68 mS/m also indicated a very high water content. The standard deviation of EC_a on this day (4.51 mS/m) was substantially greater than on August 12 or August 14, possibly implying that soil moisture conditions were less uniform across the test plot. Furthermore, all four of the drain lines were filled with water. Consequently, the observations imply very wet test plot soil conditions on August 13 after sprinkler irrigation, with a water table level that was likely at or near the ground surface.

Table 2. Soil radar signal velocity with associated soil dielectric constant and soil volumetric water content.

Data collection date	Soil radar signal velocity* (m/ns)	Soil dielectric constant† (dimensionless)	Soil volumetric water content‡ (dimensionless)
August 12, 2009	0.079	14.31	0.208
August 13, 2009	0.050	35.54	0.467
August 14, 2009	0.056	29.21	0.394

*Determined from reflection hyperbola curve fitting (Sensors & Software Inc., 2009).
†Calculated from soil radar velocity (Conyers, 2004).
‡Calculated from soil dielectric constant (Sutinen, 1992).

On August 14, 2009, the third set of GPR data were collected after a 24 hour period where the soil was allowed to drain. The test plot's shallow hydrologic conditions were still wet, but without standing water at the ground surface. The estimated near surface soil volumetric water content averaged 0.431. A relatively large test plot EC_a value of 27.57 mS/m indicates that the soil still had a very high water content (Table 1). The standard deviation of EC_a on this day (2.39 mS/m) was fairly small, possibly implying that soil moisture conditions were fairly uniform across the test plot. All four of the recently installed drain lines were mostly to completely empty of water on the far west side of the test plot and mostly to completely full of water on the far east side. Consequently, the test plot was determined to have very wet soil conditions on August 14, with a water table level that likely had drained to a depth near that of the recently installed drain lines (~0.6 m).

Ground Penetrating Radar Results - Moderately Dry Soil Conditions (August 12, 2009)

Reflection hyperbola curve fitting (Sensors & Software Inc., 2009) of the August 12, 2009 GPR data determined that the bulk soil radar velocity on that day was 0.079 m/ns (Table 2). This bulk radar velocity value is representative of a portion of the soil profile from the ground surface down to the top of the drain lines (~0.5-m depth). The soil dielectric constant calculated from this radar velocity (Conyers, 2004) is 14.31, while the volumetric water content calculated from the dielectric constant (Sutinen, 1992) is 0.208 (Table 2). The GPR-derived volumetric water content is similar to the volumetric water content of 0.184 measured using TDR methods. The similarity and relatively low value of these two soil volumetric water contents serve to substantiate the presence of moderately dry soil conditions.

It is estimated that the drainage pipe, if comprised of dry clay tile, would probably have a dielectric constant ranging from 3 to 7 based on documented values for dry clay sediments, aluminosilicate minerals, and fired porcelain ceramics (Chemical Rubber Company, 1994; Sharma, 1997; VIAS Encyclopedia, 2010). However, if clay tile is capable of adsorbing water, then it would likely have a dielectric constant similar to that of the surrounding soil. The dielectric constant of the CPT drainage pipe has a value averaging 2.35 (Chemical Rubber Company, 1994). The air within these dry pipes has a dielectric of 1. Consequently, there are fairly large differences between the dielectric constants of the drainage pipes or the air within the pipes versus the moderately dry soil dielectric constant value of 14.31, and this contrast allowed for detectable responses on August 12.

Results of a study by Allred *et al.* (2005b) indicated that the type of drainage pipe present, either clay tile or CPT, does not seem to impact the GPR drainage pipe response. The GPR drainage pipe response, in fact, seemed to be most influenced by the dielectric constant contrast between the soil surrounding the pipe and the air or water inside the pipe. This finding is supported by Zeng and McMechan (1997) who found similar results with buried plastic pipes.

Representative GPR profile and amplitude map results from August 12 are shown in Fig. 3 (antennas oriented parallel to the drain lines) and Fig. 4 (antennas oriented perpendicular to the drain lines). The Fig. 3(b) and Fig. 4(b) south-to-north GPR profiles were acquired 1.2 m to the east of the west boundary. The strongest GPR reflection hyperbola drainage pipe responses (upside down U-shaped features) were generally found with data collected using antennas perpendicular to the drain lines (as in Fig. 4(b)) rather than antennas parallel to the drain lines (as in Fig. 3(b)). For example, the reflection hyperbolae for Pipes 2, 4, A, and B are stronger in Fig. 4(b) than in Fig. 3(b), whereas the strength of the responses for Pipe 1 and Pipe 3 are about the same in both figures. Overall, the scaled, signal enhanced (gained) maximum GPR drainage pipe response amplitudes for Pipes 1, 2, 3, 4, A, and B were on average 50% greater in Fig. 4(b) than Fig. 3(b).

The GPR amplitude maps in Figs. 3(c) and 4(c) represent reflected radar energy from a depth interval of

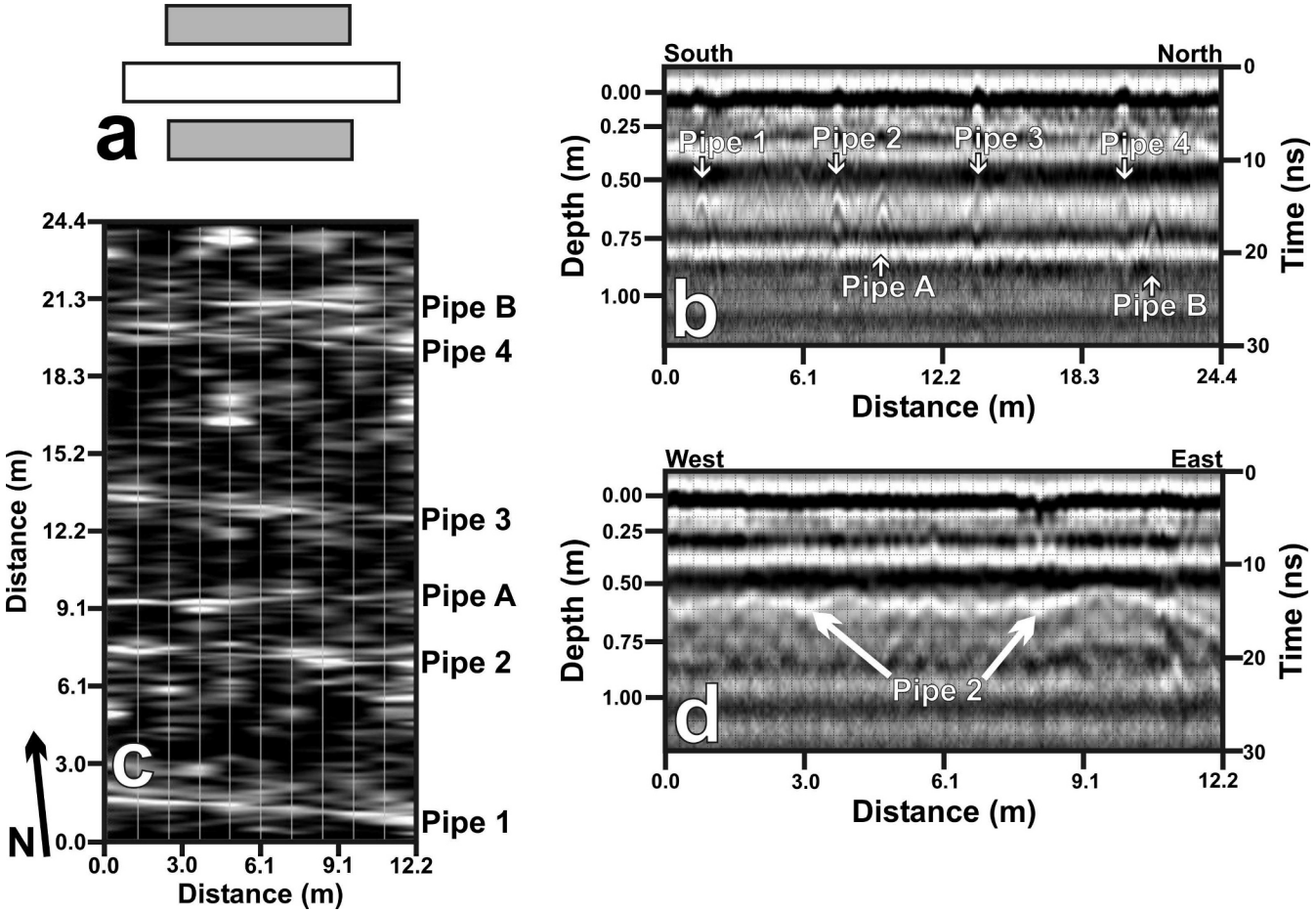

Figure 3. Representative August 12 GPR results under moderately dry soil conditions with antennas oriented parallel to drain line direction. a) Schematic showing orientation of antennas (gray bars) relative to drainage pipe (white bar), b) south-to-north GPR profile from measurement transect 1.2-m east of west test plot boundary, c) GPR amplitude map for 0.46 m to 0.76 m depth interval, and d) GPR profile from measurement transect directly over top and along trend of Pipe 2. GPR profile and map depths are based on a soil radar velocity of 0.079 m/ns.

0.46 m to 0.76 m. The figures show that there are stronger and/or more distinct GPR drainage pipe responses (lighter shaded linear features) found with GPR data collected using antennas perpendicular to the drain lines (Fig. 4(c)) rather than antennas parallel to the drain lines (Fig. 3(c)). In particular, Pipes 2, 4, A, and B are better delineated in Fig. 4(c) than in Fig. 3(c), while the Pipes 1 and 3 are delineated equally well in both.

August 12 GPR data were also collected along measurement transects directly over top and along trend of Pipes 1, 2, 3, and 4. Figs. 3(d) and 4(d) show profiles collected over Pipe 2, which exhibit the typical banded linear response (Allred *et al.,* 2004; Allred *et al.,* 2005b; Allred and Redman, 2010). The Pipe 2 banded response was much stronger when antennas were oriented perpendicular to the drain line, with an average 120% greater amplitude compared to the parallel antenna orientation.

Overall, these results correspond well with the conclusions of Radzevicius and Daniels (2000), who determined that for relatively small diameter cylinders with a substantially lower dielectric constant compared to the surrounding soil, an antenna orientation perpendicular to the axis of the buried cylinder will produce a stronger reflected amplitude response than antennas oriented parallel to the buried cylinder. Note: On August 12, the soil profile was moderately dry, and its dielectric constant value (~14) was substantially greater than the dielectric constant of the air (~1) inside the pipes.

Shallow hydrologic conditions with moderately dry soil and air-filled drainage pipes occur when there has been limited rainfall and/or high rates of evapotranspiration. While these shallow hydrologic conditions are most commonly found in Midwest U.S. agricultural fields during summer and early fall, they

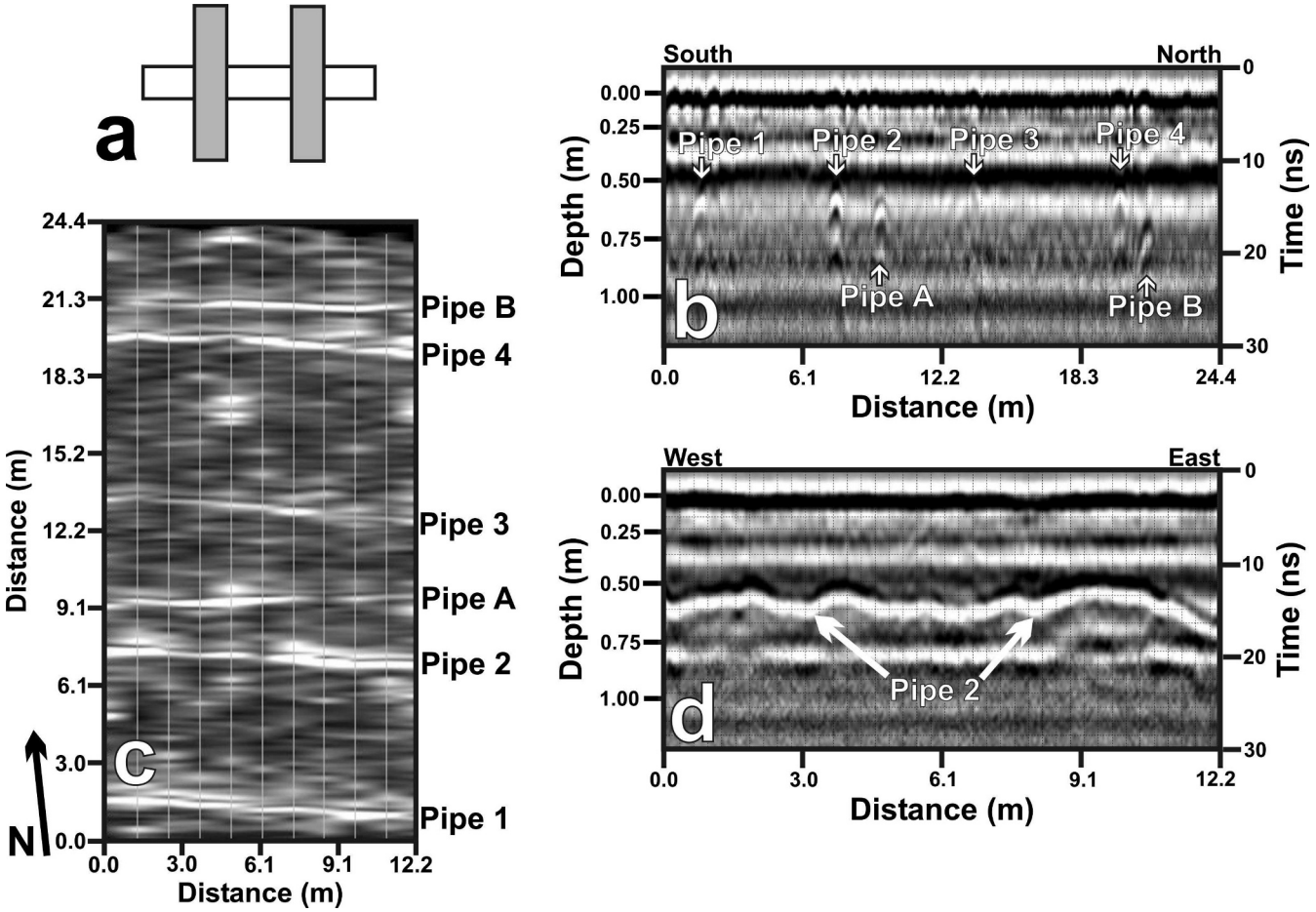

Figure 4. Representative August 12 GPR results under moderately dry soil conditions with antennas oriented perpendicular to drain line direction. a) Schematic showing orientation of antennas (gray bars) relative to drainage pipe (white bar), b) south-to-north GPR profile from measurement transect 1.2-m east of west test plot boundary, c) GPR amplitude map for 0.46 m to 0.76 m depth interval, and d) GPR profile from measurement transect directly over top and along trend of Pipe 2. GPR profile and map depths are based on a soil radar velocity of 0.079 m/ns.

can also be present in these agricultural fields at other times of the year. Consequently, if possible, given some minimal knowledge of the general directional trend for drain lines in a farm field, GPR antennas should be oriented perpendicular to the drain lines when collecting GPR drainage pipe detection data during times of the year when shallow hydrologic conditions are characterized by moderately dry soils and air-filled drainage pipes.

Ground Penetrating Radar Results – Saturated Wet Soil Conditions (August 13, 2009)

Reflection hyperbola curve fitting revealed that the soil radar velocity on August 13, 2009 was 0.050 m/ns (Table 2). In turn, the soil dielectric constant and soil volumetric water content based on the soil radar velocity of 0.050 m/ns were calculated to be 35.54 and 0.467, respectively (Table 2). The GPR-determined volumetric water content (0.467) is very similar in value to that estimated from oven drying of soil samples (0.470). The water, which filled the pipes on August 13, 2009, had a dielectric constant (~80) that was substantially different than that of the soil surrounding the drainage pipes. Consequently, this dielectric constant contrast between the water in the pipes and the soil outside the pipes provided detectable GPR pipe responses.

Amplitude maps and representative GPR profiles for the August 13 data are shown in Figs. 5 and 6. The Fig. 5 results are representative of data collected with GPR antennas oriented parallel to the drain lines, while the Fig. 6 results are representative of data collected with antennas oriented perpendicular to the drain lines. The location of the profiles in Fig. 5(b) and Fig. 6(b) were the same as that in Figs. 3(b) and 4(b). The strongest GPR reflection hyperbola drainage pipe

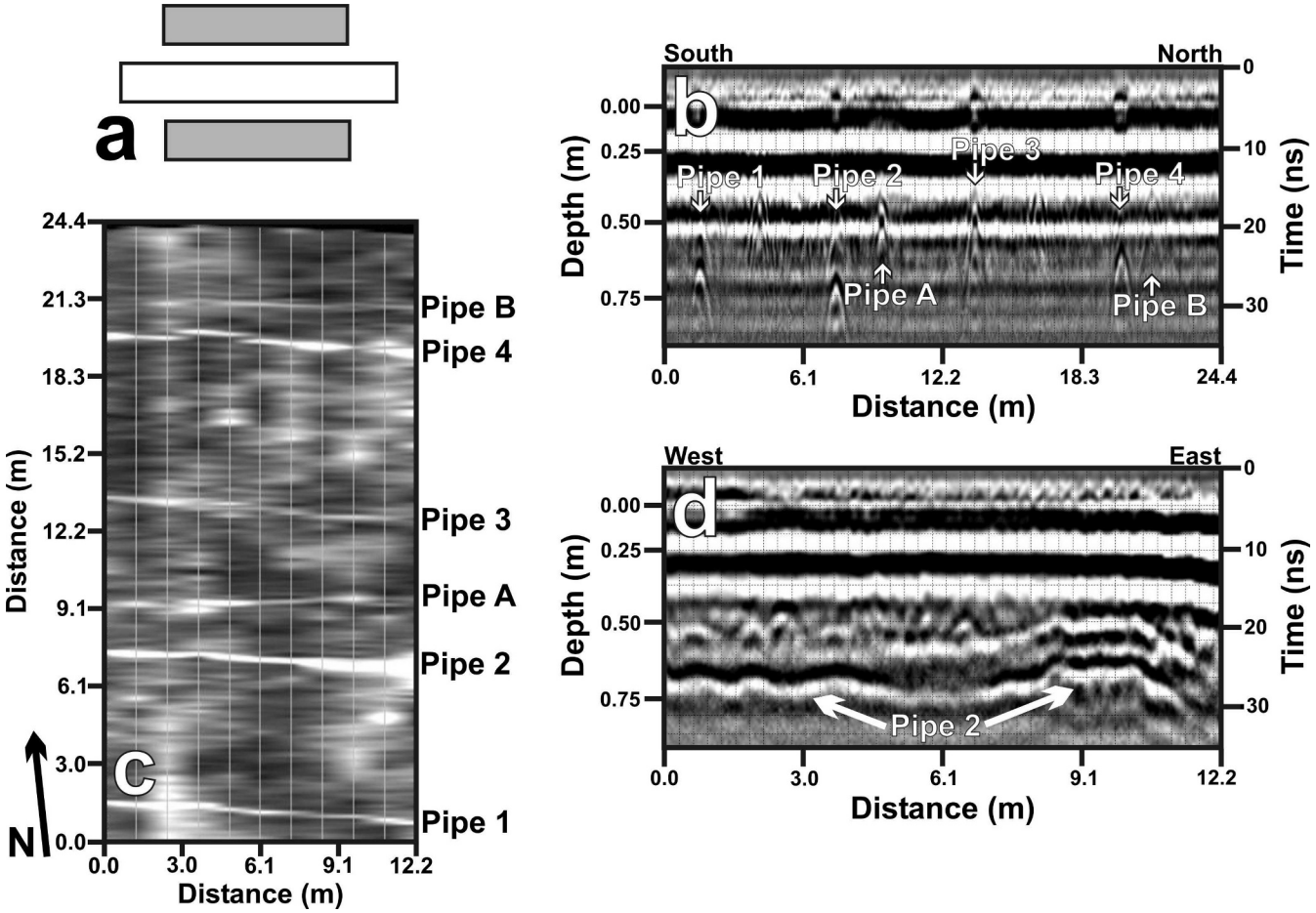

Figure 5. Representative August 13 GPR results under saturated wet soil conditions with antennas oriented parallel to drain line direction. a) Schematic showing orientation of antennas (gray bars) relative to drainage pipe (white bar), b) south-to-north GPR profile from measurement transect 1.2-m east of west test plot boundary, c) GPR amplitude map for 0.46 m to 0.76 m depth interval, and d) GPR profile from measurement transect directly over top and along trend of Pipe 2. GPR profile and map depths are based on a soil radar velocity of 0.050 m/ns.

responses on August 13 were generally found with the antennas parallel to the drain lines (Fig. 5(b)) rather than perpendicular to the drain lines (Fig. 6(b)). Overall, the GPR drainage pipe response amplitudes for Pipes 1, 2, 3, 4, A, and B were around 25% greater in Fig. 5(b) than Fig. 6(b).

It is interesting to note that dual upper and lower reflection hyperbola drainage pipe responses are commonly found on the August 13 and August 14 south-to-north GPR profiles generated from data collected with the antennas oriented parallel to the drain lines. Why these dual reflection hyperbola responses were not found on the August 13 and August 14 south-to-north GPR profiles generated from data collected with the antennas oriented perpendicular to the drain lines is unclear. Generally, the lower reflection hyperbola response is stronger than the upper hyperbola. A dual reflection hyperbola response is explained by first considering the fact that radar waves pass from the side of the drainage pipe closest to the GPR antennas, through the air/water/soil-filled pipe interior, to the other side of the drainage pipe furthest from the GPR antennas, in turn producing reflected radar signals from both sides of the pipe. If the radar signals reflected from both sides of the pipe are strong and there is sufficient separation in their arrival time at the receiving antenna, then an upper and lower reflection hyperbola response should be anticipated. When only air is present inside the pipe, as was generally the case on August 12, the radar wave velocity through the pipe interior is large enough that there is very little time separation between the radar signals reflected from both sides of the pipe, and in actuality, the time separation between the two reflected radar signals is so small that the two signals become superimposed on one another (*e.g.,* Pipe 2 in Figs. 3(b) and 4(b)). For the same reason, pipes filled

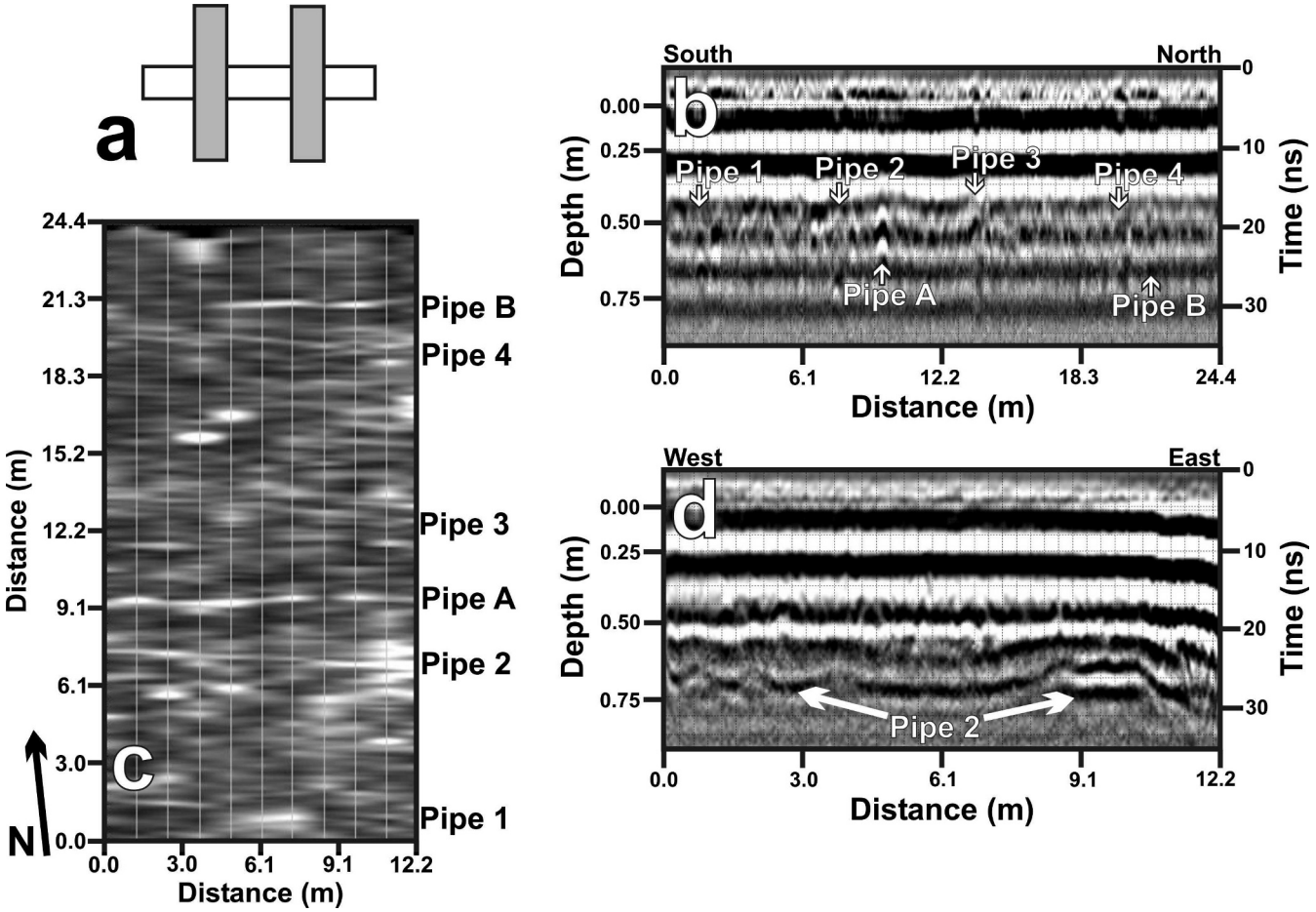

Figure 6. Representative August 13 GPR results under saturated wet soil conditions with antennas oriented perpendicular to drain line direction. a) Schematic showing orientation of antennas (gray bars) relative to drainage pipe (white bar), b) south-to-north GPR profile from measurement transect 1.2-m east of west test plot boundary, c) GPR amplitude map for 0.46 m to 0.76 m depth interval, and d) GPR profile from measurement transect directly over top and along trend of Pipe 2. GPR profile and map depths are based on a soil radar velocity of 0.050 m/ns.

with an air/soil combination or a water/soil combination will also likely produce what appears to be a single reflection hyperbola response (*e.g.,* Pipe 3). Conversely, when water only completely fills the inside of the pipe, the radar wave velocity through the pipe interior is slow enough that there is sufficient time separation between the radar signals reflected from both sides of the pipe, and there is no interference between the two reflected radar signals, thus resulting in a dual reflection hyperbola response as shown for Pipes 1 and 2 in Fig. 5(b).

The August 13 GPR amplitude maps (depth interval of 0.46 to 0.76 m) are shown in Figs. 5(c) and 6(c). As depicted, there are stronger and/or more distinct GPR drainage pipe responses (lighter shaded linear features) found with GPR data collected using antennas parallel to the drain lines (Fig. 5(c)) rather than perpendicular to the drain lines (Fig. 6(c)). In particular, Pipes 1, 2, 3, and 4 are better delineated in Fig. 5(c), while the Pipes A and B are delineated equally well in both Figs. 5(c) and 6(c). Figures 5(d) and 6(d) are GPR profiles over top and along trend of Pipe 2. The banded linear response for Pipe 2 was stronger (by 15%) when antennas were oriented parallel to the drain line than when the antennas were oriented perpendicular to the drain line.

In summary, GPR drainage pipe responses on August 13 were significantly stronger with GPR antennas oriented parallel to the drain lines than with GPR antennas oriented perpendicular to the drain lines. This finding is reversed from that of August 12, when soil conditions were much drier. This result corresponds well with the conclusion of Radzevicius and Daniels (2000) that for relatively small diameter cylinders buried beneath the ground surface, if the dielectric constant of the cylinder (essentially comprised of water in this

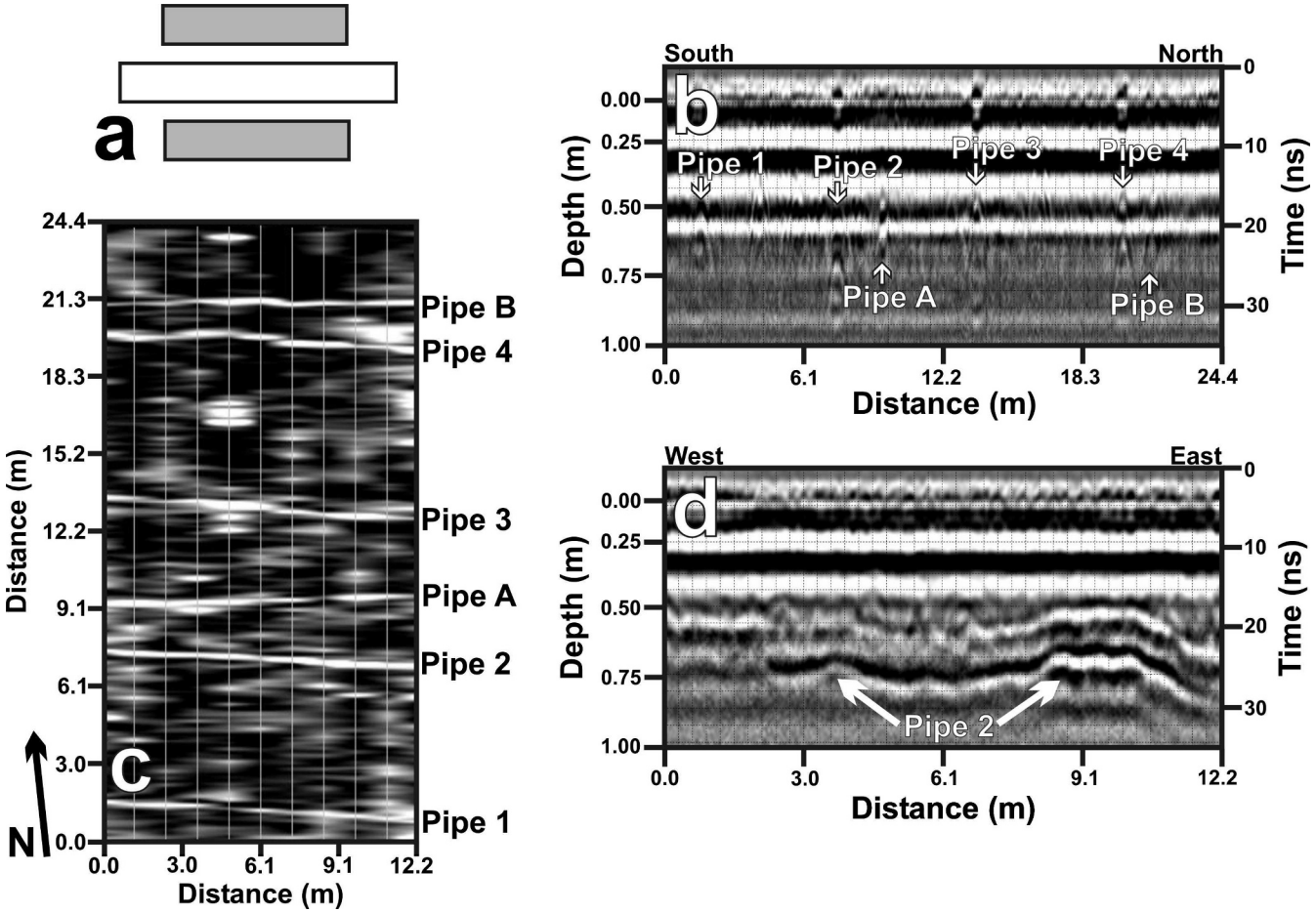

Figure 7. Representative August 14 GPR results under drained wet soil conditions with antennas oriented parallel to drain line direction. a) Schematic showing orientation of antennas (gray bars) relative to drainage pipe (white bar), b) south-to-north GPR profile from measurement transect 1.2-m east of west test plot boundary, c) GPR amplitude map for 0.46 m to 0.76 m depth interval, and d) GPR profile from measurement transect directly over top and along trend of Pipe 2. GPR profile and map depths are based on a soil radar velocity of 0.056 m/ns.

case) is substantially more that the dielectric constant of the surrounding soil, then a GPR transmitting/receiving antenna orientation parallel to the axis of the buried cylinder will produce a stronger GPR response than a transmitting/receiving antenna orientation perpendicular to the axis of the buried cylinder. On August 13, the soil profile was very wet, and its dielectric constant value (35.54) was substantially less than the dielectric constant of the water inside the pipes (80).

Shallow hydrologic conditions with very wet soil and water-filled drainage pipes occur during and directly following large rainfall events. While these shallow hydrologic conditions are most commonly found in Midwest U.S. agricultural fields during late fall, winter, and spring, they can also be present in these agricultural fields at other times of the year. Consequently, if possible, given some minimal knowledge of the general directional trend for drain lines in a farm field, GPR antennas should be oriented parallel to the drain lines when collecting GPR drainage pipe location and functionality assessment data during times of the year when shallow hydrologic conditions are characterized by very wet soils and water-filled drainage pipes.

Ground Penetrating Radar Results - Drained Wet Soil Conditions (August 14, 2009)

Reflection hyperbola curve fitting of the August 14, 2009 GPR data determined that the soil radar velocity was 0.056 m/ns. This velocity value was used to calculate a soil dielectric constant of 29.2 and a volumetric water content of 0.394. Again, these Table 2 values of soil radar velocity, soil dielectric constant, and soil volumetric water content are all bulk values representative of a portion of the soil profile from the ground surface down to the top of the drain lines. The August 14 soil volumetric water content of 0.394

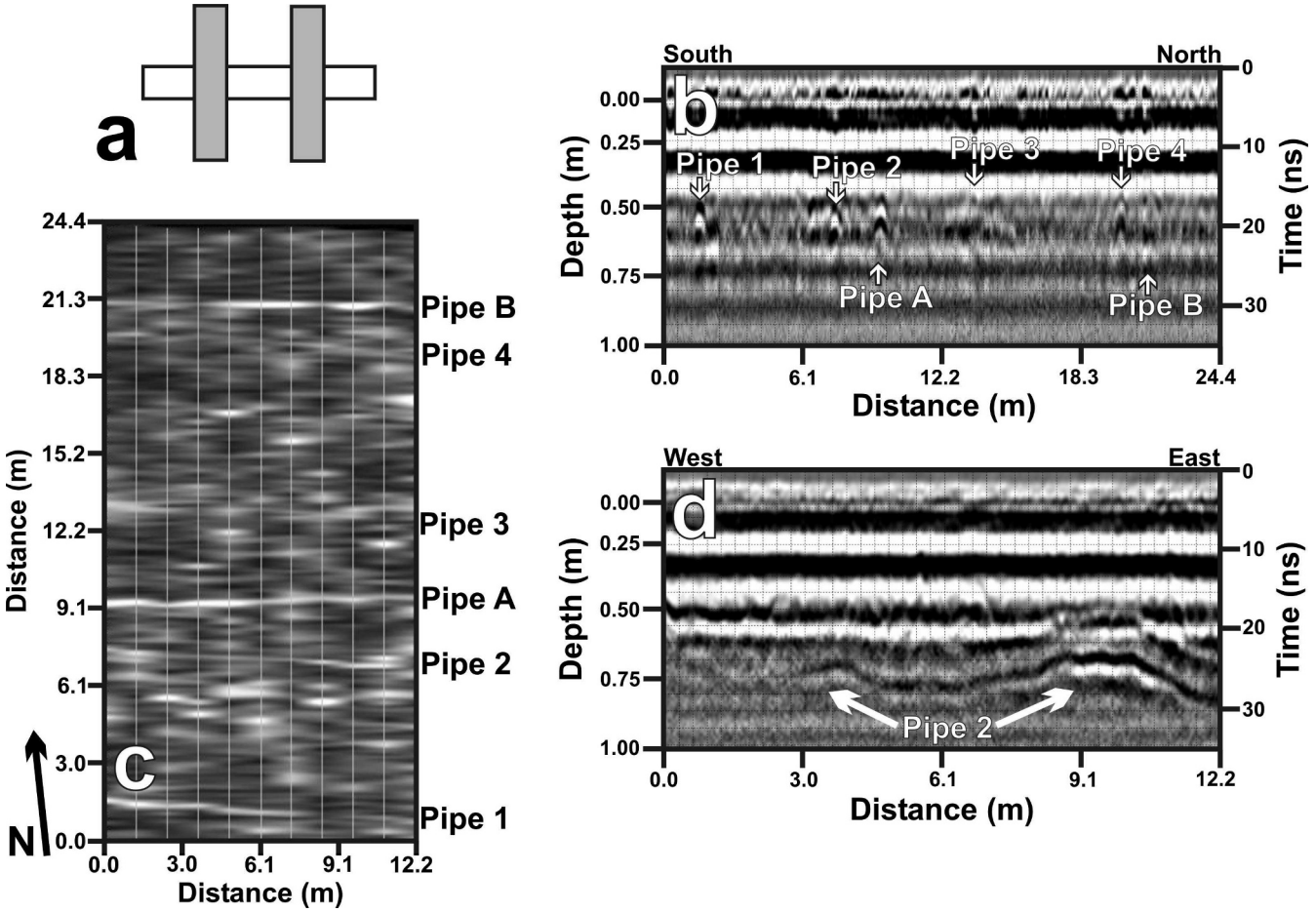

Figure 8. Representative August 14 GPR results under drained wet soil conditions with antennas oriented perpendicular to drain line direction. a) Schematic showing orientation of antennas (gray bars) relative to drainage pipe (white bar), b) south-to-north GPR profile from measurement transect 1.2-m east of west test plot boundary, c) GPR amplitude map for 0.46 m to 0.76 m depth interval, and d) GPR profile from measurement transect directly over top and along trend of Pipe 2. GPR profile and map depths are based on a soil radar velocity of 0.056 m/ns.

calculated from the soil dielectric constant is similar in value to the August 14 near-surface soil volumetric water content of 0.431 (Table 1) estimated from oven drying of soil samples. Furthermore, on this day, the water table level was near the depth of the drain lines, which were mostly empty on the far west side and mostly full of water on the far east side of the test plot. Consequently, on August 14, there were fairly large differences in the dielectric constant between the surrounding soil (29.2) and the air (1) and/or water (80) inside the pipes, thereby allowing for detectable GPR drainage pipe responses.

Amplitude maps and representative GPR profiles for August 14 are shown in Figs. 7 and 8. For south-to-north GPR profiles, which are oriented 90° to the test plot drain lines, the GPR reflection hyperbola drainage pipe responses were marginally more distinct with parallel antennas (as in Fig. 7(b)) compared to perpendicular antennas (as in Fig. 8(b)). For example, Pipes 1, 2, 3, and 4 are somewhat clearer in Fig. 7(b) than in Fig. 8(b), while the strength of the GPR drainage pipe responses for Pipes A and B are about the same in both figures. Overall, when comparing Fig. 7(b) to Fig. 8(b), the pipe response amplitudes are, on average, very similar for both orientations.

The GPR amplitude maps (Figs. 7(c) and 8(c)), which are indicative of the amount of reflected radar energy from a depth interval of 0.46 to 0.76 m, show that there are stronger and/or more distinct pipe responses (lighter shaded linear features) with antennas parallel to the drain lines (Fig. 7(c)) compared to antennas perpendicular to the drain lines (Fig. 8(c)). In particular, Pipes 1, 2, 3, and 4 are better delineated in Fig. 7(c), while the Pipes A and B are delineated equally well in both Figs. 7(c) and 8(c). Figs. 7(d) and 8(d) are GPR profiles collected over top and along trend of Pipe

2. The banded linear drainage pipe response for Pipe 2 depicted on these GPR profiles was marginally stronger (averaged 10% greater amplitude) when antennas were oriented parallel to the drain line than when oriented perpendicular to the drain line.

In summary, similar to August 13, but to a lesser extent, the GPR drainage pipe responses on August 14 were marginally stronger and/or more distinct with GPR antennas oriented parallel to the drain lines than with GPR antennas oriented perpendicular to the drain lines. Again, this finding is reversed from that of August 12, when soil conditions were much drier. On August 14, the soil was wet and the drainage pipes partially filled with water.

Shallow hydrologic conditions with very wet soil and partially water-filled drainage pipes typically will occur a few hours or days shortly after large rainfall events, once the soil has had a chance to drain. While these shallow hydrologic conditions are most commonly found in Midwest U.S. agricultural fields during late fall, winter, and spring, they can also be present in these agricultural fields at other times of the year. Consequently, if possible, given these shallow hydrologic conditions (wet, drained) and some minimal knowledge of the general directional trend for drain lines in a farm field, GPR antennas should be oriented parallel to the drain lines when collecting GPR drainage pipe location and functionality assessment data.

Synopsis, Conclusions, and Future Work

A field research study was carried out at a specially designed test plot to evaluate the effect on ground penetrating radar drainage pipe detection caused by the antenna-to-pipe orientation. Antenna orientations perpendicular and parallel to drain lines were tested using 250 MHz antennas. Ground penetrating radar data were collected under dry and wet shallow hydrologic conditions. The major findings of this investigation include the following:

1) Antennas perpendicular to the drain lines provide the strongest GPR drainage pipe response for agricultural field conditions with moderately dry soils and empty, air-filled drainage pipes, such as would be present during periods of limited rainfall and high evapotranspiration rates.
2) Antennas parallel to the drain lines provide the strongest GPR drainage pipe response for agricultural field conditions with very wet soils and water-filled drainage pipes, such as would occur during and directly following large rainfall events.
3) Antennas parallel to the drain lines provide a marginally better GPR drainage pipe response for agricultural field conditions with very wet soils and partially water-filled drainage pipes, such as would occur a few hours or days shortly after large rainfall events, once the soil has had a chance to drain.

Consequently, given a general estimation of shallow hydrologic conditions and some basic knowledge of drain line directional trends in an agricultural field (information that is often available through simple measurements, site inspections, or farmer input), the best GPR antenna orientation relative to the drain lines (parallel or perpendicular) and GPR survey plan can be chosen to maximize the data quality for GPR drainage pipe location and functionality assessment. Although the results of this case study provide some very useful information regarding GPR antenna set-up when using GPR methods to locate and evaluate agricultural field drainage pipes, there is still a need for further investigation. Specifically, different antenna configurations relative to a drain line and different antenna frequencies should be examined, along with thorough testing of the antenna-to-pipe orientation impacts on the GPR drainage pipe response in a variety of diverse soil types.

Author's Note

The use of equipment manufacturer names are provided for informational purposes only and does not imply endorsement by the author or the USDA – Agricultural Research Service.

References

Allred, B.J., Fausey, N.R., Peters Jr., L., Chen, C., Daniels, J.J., and Youn, H., 2004, Detection of buried agricultural drainage pipe with geophysical methods: Applied Engineering in Agriculture, **20**, 307–318.

Allred, B.J., Redman, J.D., McCoy, E.L., and Taylor, R.S., 2005a, Golf course applications of near-surface geophysical methods: A case study: Journal of Environmental and Engineering Geophysics, **10**, 1–19.

Allred, B.J., Daniels, J.J., Fausey, N.R., Chen, C., Peters Jr., L., and Youn, H., 2005b, Important considerations for locating buried agricultural drainage pipe using ground penetrating radar: Applied Engineering in Agriculture, **21**, 71–87.

Allred, B.J., and Redman, J.D., 2010, Location of agricultural drainage pipes and assessment of agricultural drainage pipe conditions using ground penetrating radar: Journal of Environmental and Engineering Geophysics, **15**, 119–134.

Boniak, R., Chong, S.K., Indorante, S.J., and Doolittle, J.A., 2002, Mapping golf course green drainage systems and subsurface features using ground penetrating radar: *in* Koppenjan, S.K., and Lee, H. (eds.), Proceedings of

SPIE, Vol. 4758: Ninth International Conference on Ground Penetrating Radar, International Society of Optical Engineering, Bellingham, Washington, 477–481.

Chow, T.L., and Rees, H.W., 1989, Identification of subsurface drain locations with ground-penetrating radar: Canadian Journal of Soil Science, **69**, 223–234.

Conyers, L.B., 2004. Ground-penetrating radar for archaeology, AltaMira Press, Walnut Creek, California.

Chemical Rubber Company, 1994, CRC Handbook of chemistry and physics: Lide, D.R. (ed.), CRC Press, Boca Raton, Florida.

Hayakawa, H., and Kawanaka, A., 1998, Radar imaging of underground pipes by automated estimation of velocity distribution versus depth: J. Applied Geophysics, **40**, 37–48.

Hillel, D., 1980. Fundamental of soil physics, Academic Press, Inc., San Diego, California.

LaFaleche, P.T., Todoeschuck, J.P., Jensen, O.G., and Judge, A.S., 1991, Analysis of ground probing radar data: Predictive deconvolution: Canadian Geotechnical Journal, **28**, 134–139.

McNeill, J.D., 1980. Electromagnetic terrain conductivity measurement at low induction numbers, Technical Note TN-6, Geonics Limited, Mississauga, Ontario, Canada.

National Climate Data Center, 2009, Climatological Data – Ohio – August 2009: Volume 114, Number 8, ISSN 0364-558, National Atmospheric and Oceanic Administration, Ashville, North Carolina.

Pavelis, G.A., 1987, Economic survey of farm drainage: *in* Pavelis, G. (ed.), Farm Drainage in the United States: History, Status, and Prospects: Miscellaneous Publication Number 1455, U.S. Dept. of Agriculture, Economic Research Service, Washington, D.C., 110–136.

Peters Jr., L., and Young, J.D., 1986, Applications of subsurface transient radar: *in* Miller, E.K. (ed.), Time Domain Measurements in Electromagnetics: Van Nostrand Reinhold, New York, New York, 297–351.

Radzevicius, S.J., and Daniels, J.J., 2000, Ground penetrating radar polarization and scattering from cylinders: Journal of Applied Geophysics, **45**, 111–125.

Roberts, R., and Daniels, J.J., 1996, Analysis of GPR polarization phenomena: Journal of Environmental and Engineering Geophysics, **1**, 139–157.

Sensors and Software Inc., 2009, EKKO_Mapper user's guide, Sensors & Software Inc., Mississauga, Ontario, Canada.

Sharma, P.V., 1997. Environmental and engineering geophysics, Cambridge University Press, Cambridge, United Kingdom.

Streich, R., van der Kruk, J., and Grasmueck, M., 2008, Polarization effects of buried pipes in vector-migrated 3-D ground-penetrating radar data: *in* Proceedings of the 12th International Conference on Ground Penetrating Radar, June 16–19, Birmingham, UK, 6 pp.

Sutinen, R., 1992. Glacial deposits, their electrical properties and surveying by image interpretation and ground penetrating radar: Bulletin 359, Geological Survey of Finland, Rovaniemi, Finland.

VIAS Encyclopedia, 2010, http://www.vias.org/encyclopedia/phys_dielectric_const.htm.

Wensink, W.A., Hofman, J., and Van Deen, J.K., 1991, Measured reflection strengths of underwater pipes irradiated by pulsed horizontal dipole in air: Comparison with continuous plane-wave scattering theory: Geophysical Prospecting, **39**, 543–566.

Wray, W.K., 1986. Measuring engineering properties of soil: Prentice-Hall, Inc., Englewood Cliffs, New Jersey.

Zeng, X., and McMechan, G.A., 1997, GPR characterization of buried tanks and pipes: Geophysics, **62**, 797–806.